Semiconductor Physics, Quantum Electronics & Optoelectronics, 2023. V. 26, No 2. P. 180-187.

Optics

Narrow-band controllable sources of IR emission based on one-dimensional magneto-optical photonic structures

E.F. Venger, V.O. Morozhenko*

V. Lashkaryov Institute of Semiconductor Physics, NAS of Ukraine, 41, prosp. Nauky, 03680 Kyiv, Ukraine
**Corresponding author e-mail: morozh@meta.ua*

Abstract. Creation of controllable narrow-band emission sources for the mid- and long-wavelength infrared ranges is one of the primary tasks of infrared technology. In this paper, we propose and demonstrate non-luminescent (thermal) magnetically controllable sources of infrared emission based on semiconductor magneto-optical photonic structures (MOPS). It is shown that interference effects cause narrow-band thermal emission spectrum of such sources, and magnetic field makes it possible to effectively control the spectral and amplitude characteristics of emissivity in the mid- and long-wavelength infrared range. Influence of the MOPS composition and design on the source emissive characteristics is studied. Using the obtained results, the designs of A^3B^5 semiconductor compounds based sources with dynamically tunable spectrum and amplitude modulation of emission are proposed. Theoretical modeling has shown the possibility of dynamic control of their emission parameters by achievable magnetic fields. Such sources may be used in environmental monitoring systems, medicine, forensics, infrared spectroscopy, *etc*.

Keywords: infrared sources, magneto-optical photonic structures, thermal emission, emissivity.

https://doi.org/10.15407/spqeo26.02.180
PACS 85.30.De, 85.60.Jb

Manuscript received 07.02.23; revised version received 11.04.23; accepted for publication 07.06.23; published online 26.06.23.

1. Introduction

At present, infrared (IR) emission sources are widely used in scientific research, gas analysis systems, spectroscopy, medicine, *etc*. Use of the mid-wavelength (MWIR) and long-wavelength (LWIR) IR spectral regions significantly expands the scope of application of optical devices due to the following reasons: these regions comprise the atmospheric-transmission bands, many substances have characteristic absorption lines in these spectral regions, these regions account for the maximum of thermal emission of objects with the temperature of 10…50 °C, which is relevant for a number of analysis, control and monitoring systems.

Modern optical IR systems need controllable narrow-band sources of IR emission, *i.e*. those that can operate in pulsed or pulse-frequency modes. Of special interest are also the sources enabling smooth tuning of their spectral characteristics. Although LEDs operating in the near-infrared ($\lambda < 2$ μm) region are successfully used, their quantum yield sharply decreases in the MWIR and LWIR ranges. Application of quantum wells and super-lattices makes it possible to shift the LED spectral characteristics to longer wavelengths (up to $\lambda \approx 10$ μm) [1–4] and even to create LEDs with a two-color spectral characteristic [5, 6]. However, such LEDs operate at cryogenic temperatures, which makes their application difficult.

A promising field is application of non-luminescent (thermal) sources of IR emission, the emission intensity of which can be controlled by changing their emissivity. In [7, 8], semiconductor IR sources with dynamic intensity control by changing the concentration of free charge carriers by contact injection [7] or illumination [8] were investigated and proposed. The advantage of IR sources is that they do not require additional means of intensity modulation. However, they have a broad ($\lambda \approx 3…18$ μm) spectrum. Therefore, additional filters are needed when narrow-band emission is required.

A new potential for realizing thermal type controllable narrow-band IR sources is provided by photonic structures (PS) used as the emission elements. These structures can produce highly directional thermal emission in a narrow spectral range and, with a matching design of PS, the emission line intensity can practically achieve the intensity of the blackbody emission. To date,

a large number of such structures have been synthesized and investigated with that end in view. PS such as photonic crystals [9–12], resonant cavities and layered structures [13–18] have been proposed as the narrow-band IR sources for MWIR and LWIR spectral regions. If one or more PS layers have non-zero absorption, the heated PS emits in the spectral region of a pass band. In the framework of classical optics, the coherent peculiarities of their thermal emission (TE) are explained by multi-beam interference of light spontaneously emitted in the structure. The TE spectral and amplitude characteristics of such emitters are defined by the layer parameters and the PS design. A number of them [9–13] are the sources of invariable emission (without possibility of dynamic control of the spectrum or amplitude).

Use of materials, the properties of which can be changed by some external influences, makes it possible to change the PS optical characteristics and to control its TE characteristics. In [14–16], the possibility of changing the emission characteristics of PS containing a layer of phase-changing material (PCM) was studied. It was shown that the emissivity of such structures can be changed by changing the PCM phases by heating. However, in authors' opinion, use of heating for dynamic control of the parameters of thermal IR emitters is difficult to implement in a finished product provided its stability is ensured. In [17], a narrow-band emitter operating in the LWIR range and enabling dynamic intensity control by external illumination was described. The emitter was based on a metamaterial consisting of the matrix of the resonant cavities filled with photosensitive material ZnO. The device included an ultraviolet light source that illuminated this metamaterial. The emission intensity of the IR emitter was controlled by the intensity of the ultraviolet light, which changed the transmittance of ZnO and, with it, the Q factor of the resonant cavities.

It was experimentally discovered in [18] that the TE spectrum of a magnetophotonic layer changes significantly in a magnetic field. Both the disappearance of emission lines and their inversion in the spectrum were observed. In [19], it was determined that magnetic field leads to the deformation of the directional diagram of TE as well. Based on the obtained results, the authors concluded that use of magneto-optical photonic structures (MOPS) is promising for creating controllable narrow-band emission sources in the MWIR and LWIR spectral regions.

This paper theoretically investigates the possibility of using one-dimensional MOPS as the controllable narrow-band sources of IR emission in the MWIR and LWIR spectral regions with the possibility of dynamic control of their emission characteristics. The dependence of the emission parameters of such sources on the optical characteristics and design features of the emitting structure is studied. Based on the obtained results, designs of magnetic field controllable emission sources with tunable spectral characteristics and dynamic amplitude modulation are presented.

2. Model and basic relations

Consider an emitter that consists of a 1-D magneto-photonic structure placed on a finite incoherent substrate as shown schematically in Fig. 1. MOPS includes a magneto-optical layer (MOL) sandwiched between two one-dimensional stacks, which are built by superposing layers of two different dielectric materials A and B. The materials are characterized by the isotropic real refractive indexes n_A and n_B and thicknesses d_A and d_B, respectively. These stacks form the Bragg mirrors R_1 and R_2, respectively.

MOL is characterized by the isotropic zero-field complex refractive index $N_{\mathrm{MOL}} = n_{\mathrm{MOL}} + i\chi_{\mathrm{MOL}}$ ($n_{\mathrm{MOL}} << \chi_{\mathrm{MOL}}$) and thickness d_{MOL}. The substrate is characterized by the complex refractive index $N_s = n_s + i\chi_s$ and thickness d_S. The external magnetic field (**H**) is directed along the normal to the layers.

For normal light incidence on the mirror R_1, the reflectance and transmittance of the emitter in the magnetic field are, respectively [11]:

$$R^{\pm} = R^{\pm}_{\mathrm{MOPS}} + \frac{(T^{\pm}_{\mathrm{MOPS}})^2 \eta_s^2 R_3}{1-\eta_s^2 R^{\pm}_{\mathrm{MOPS}} R_3}, \quad T^{\pm} = \frac{T^{\pm}_{\mathrm{MOPS}} \eta_s (1-R_3)}{1-\eta_s^2 R^{\pm}_{\mathrm{MOPS}} R_3}, \tag{1}$$

where $\eta_s = \exp(-4\pi\chi_s d_s/\lambda)$, $T^{\pm}_{\mathrm{MOPS}}$ and $R^{\pm}_{\mathrm{MOPS}}$ are the transmittance and reflectance components of MOPS in the magnetic field, respectively:

$$T^{\pm}_{\mathrm{MOPS}} = \frac{(1-R_1)(1-R_2)\eta_{\mathrm{MOL}}}{1-2G\cos 2(\delta \pm \varphi) + G^2}, \tag{2}$$

$$R^{\pm}_{\mathrm{MOPS}} = \frac{R_1 - 2G\cos 2(\delta \pm \varphi) + R_2 \eta^2_{\mathrm{MOL}}}{1-2G\cos 2(\delta \pm \varphi) + G^2}, \tag{3}$$

$\eta_{\mathrm{MOL}} = \exp(-4\pi\chi_{\mathrm{MOL}} d_{\mathrm{MOL}}/\lambda)$, $G = \eta_{\mathrm{MOL}}\sqrt{R_1 R_2}$, $\delta = 2\pi n_{\mathrm{MOL}} d_{\mathrm{MOL}}/\lambda + \Delta$, Δ is the phase change upon reflection from the Bragg mirrors R_1 and R_2, and φ is the single-trip Faraday rotation angle, respectively.

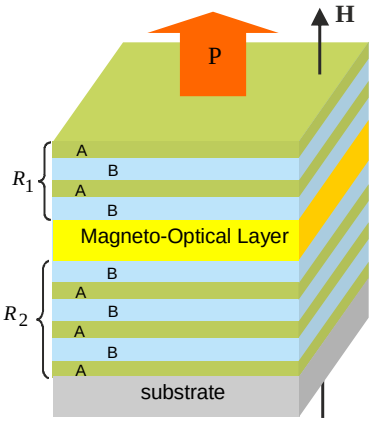

Fig. 1. Schematic of a 1-D magnetophotonic structure on a substrate.

The intensity of thermal emission of MOPS in the magnetic field coming out through the mirror R_1 normally to the surface is

$$P = P^+ + P^-, \quad (4)$$

where

$$P^{\pm} = P_{bb}\left(1 - R^{\pm} - T^{\pm}\right)/2, \quad (5)$$

and P_{bb} is the TE intensity of the blackbody under the same conditions.

3. Theoretical analysis of the emission parameters of emitter

3.1. Analysis of spectral tuning

As can be seen from Eq. (4), the thermal emission of MOPS in the magnetic field is a sum of two independent components P^- and P^+ with the narrow-band spectra. The spectral positions of the components in the absence of magnetic field coincide and correspond to the interference maximum condition $\delta = \pi k$ ($k = 1, 2, \ldots$). The lines shift in the long-wave and short-wave regions in the magnetic field, and the spectral positions of their maxima are

$$\lambda_M^{\pm} = \frac{nd}{k \pm \varphi/2\pi}. \quad (6)$$

At $\varphi = \pi/2$, other lines of the P^- and P^+ components moving toward each other merge pair-wise. It is easy to see that the spectral positions of the double lines correspond to the zero-field spectrum interference minima condition $\delta = \pi(k - 1/2)$.

Therefore, in the spectral regions between an interference maximum (λ_{M_0}) and a neighboring minimum (λ_{m_0}) of the zero-field TE spectrum, the spectral characteristic of the emitter can be smoothly tuned by changing the magnetic field. The waveband $\lambda_{M_0} \le \lambda \le \lambda_{m_0}$ (we denote it by Λ) is the maximum spectral tuning range. With further increase in the magnetic field, the process is repeated. Fig. 2 shows the dependences of Λ on the optical thickness of MOL for the lines with different interference orders k when the line is shifted in the long-wave (Fig. 2a) and short-wave (Fig. 2b) spectral regions. It can be seen from this figure that the maximum range of the emission source spectral tuning increases with the increase in the MOL optical thickness. At the same time, Λ decreases when an emission line with a higher interference order is chosen.

3.2. Dependence of the parameters of source emission line on MOPS optical characteristics

Since the emission of the source is thermal, the intensity of its TE changes with the change of emitter temperature. To eliminate the temperature dependence of the source emission characteristics, we will analyze the source emissivity $A \equiv P/P_{bb}$. In the theoretical analysis, we assume that dispersion of the refractive indices of the constituent MOPS substances is negligibly small and the reflection coefficients of the Bragg mirrors R_1 and R_2 are constant in the considered spectral range.

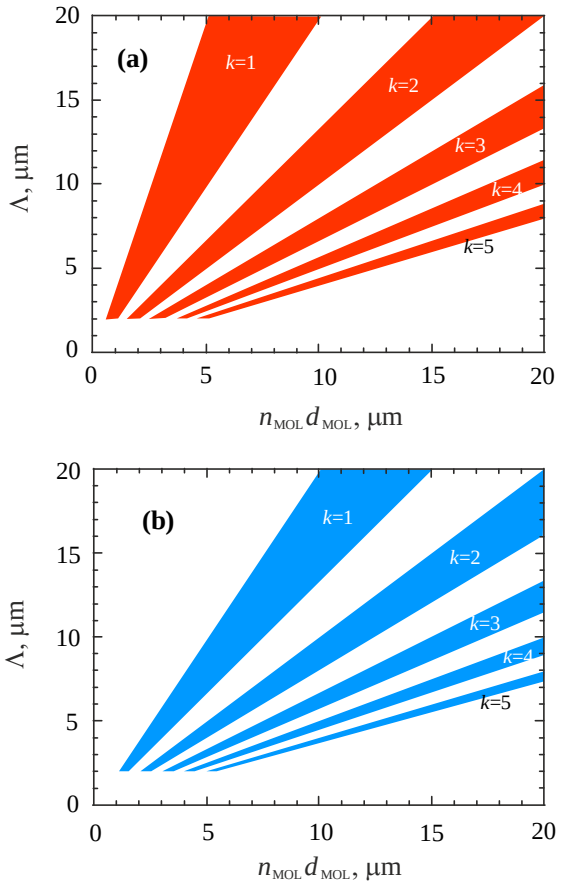

Fig. 2. Dependences of the maximum spectral tuning range of a source. As a magnetic field increases: (a) the emission line wavelength increases; (b) the emission line wavelength decreases.

We define the line height as

$$\Delta A = A_M - A_m \quad (7)$$

and consider the dependence of ΔA on the parameters of the emitter. In (7), A_M and A_m are the emissivity values in the line maximum and in the neighboring interference minimum, respectively.

Figs 3a–3c show the dependences of the line height on the two optical parameters of MOPS when the third one is constant. The substrate was supposed to be opaque ($\eta_S = 0$). As can be seen from these figures, the amplitude of the emission line strongly depends on the MOPS parameters. In contrast to non-resonant thermal emitters [7, 8], these dependences have a complex non-monotonic character. ΔA reaches its maximum value at $R_2 = 1$ (see Fig. 2a) and large values of R_1 and η_{MOL}, *i.e.* at high MOPS Q factors. At this, if R_2 may be the totally reflecting mirror ($R_2 = 1$), R_1 must be less than one.

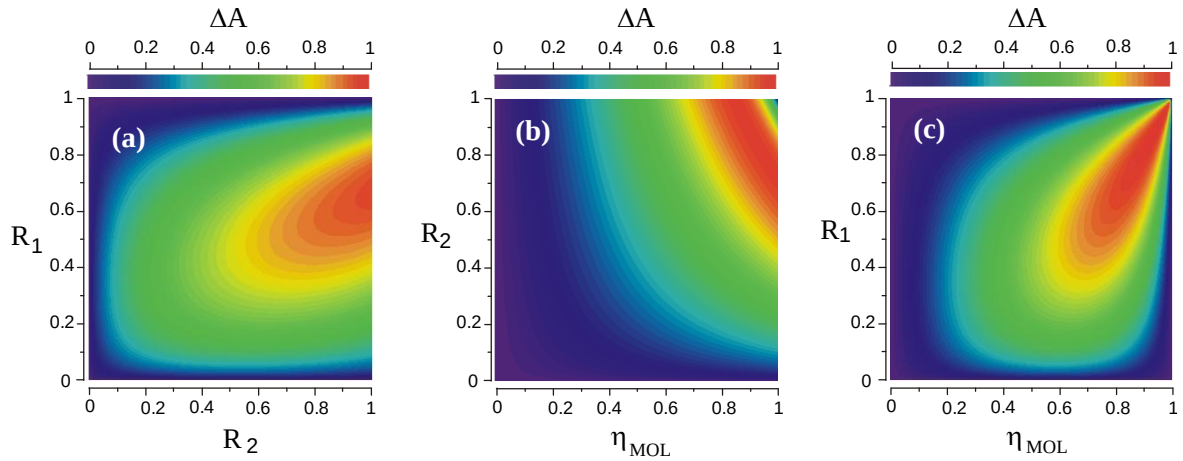

Fig. 3. Dependences of the line height on the optical parameters of MOPS on an opaque substrate ($\eta_S = 0$): (a) $\eta_{MOL} = 0.8$, (b) $R_1 = 0.7$, (c) $R_2 = 1$.

Otherwise, the emission will not be able to exit the MOPS volume. Also, the MOL absorption cannot be absent ($\eta < 1$). Otherwise, no emitting centers will be present in the MOL volume. Therefore, as can be seen in Fig. 3c, there is no emission at $\eta_{MOL} = 1$ and $R_1 = 1$.

At a high Q factor of MOPS, a compact expression for the line height can be obtained:

$$\Delta A \approx A_M = \frac{\left(1-\eta^2 R_2\right)\left(1-R_1\right)}{\left(1-G\right)^2}. \qquad (8)$$

Assuming $R_2 = 1$ and solving the differential equation $\frac{d\Delta A}{d\eta_{MOL}} = 0$, one can obtain an analytic expression that links the optimal values of R_1 and η_{MOL}, at which the intensity of the emission line is maximal and approaches the intensity of TE of the blackbody:

$$R_1 = \eta_{MOL}^2 . \qquad (9)$$

For a line width at half-amplitude, the following expression can be easily obtained:

$$\frac{\Delta\lambda}{\lambda_M} = \frac{1}{\pi k}\arccos\left(2\frac{G}{1+G^2}\right), \qquad (10)$$

where $k = 2n_{MOL}\, d_{MOL}/\lambda_M$ is an interference order of the line. At a high Q factor of MOPS, it is easy to obtain a simpler expression for $\Delta\lambda$:

$$\frac{\Delta\lambda}{\lambda_M} \approx \frac{1}{\pi k}\frac{\left(1-G\right)}{\sqrt{G}}. \qquad (11)$$

In Fig. 4, the dependence of the line width at half-amplitude on the parameter G is shown. As can be seen from this figure, $\Delta\lambda$ decreases upon improving the MOPS cavity properties. Curve *2* shows the results of the calculation according to the simplified equation (11). As it is seen, this equation is correct at $G > 0.65$.

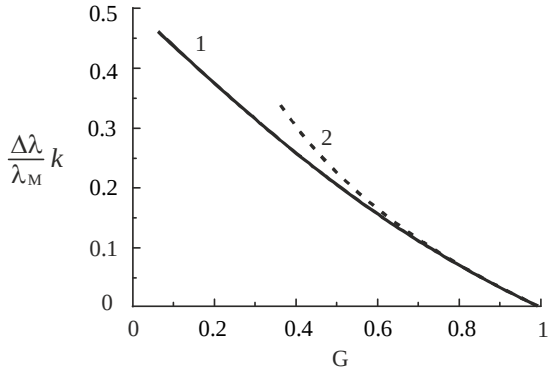

Fig. 4. Dependences of the line width at half-amplitude on the parameter $G = \eta_{MOL}\sqrt{R_1 R_2}$. *1* – calculation by the full equation; *2* – calculation by the simplified equation.

It should be noted that since the dispersion of the MOPS optical parameters was neglected deriving Eqs. (10) and (11), the value of the emission line width of a real structure may significantly differ from the calculated value.

4. Examples of the possible designs of emission sources

4.1. Emission source with spectral tuning

A design of the IR emission source with a dynamically tunable spectral characteristic, which can be implemented in practice, is shown schematically in Fig. 5. The emitter includes MOPS $(Ge/KBr)^2/InSb/(Ge/KBr)^4$ placed on a leucosapphire substrate with a heating element on the reverse side. MOPS consists of a magneto-optical InSb layer and the dielectric Bragg structures $(Ge/KBr)^2$ and $(Ge/KBr)^4$ as the mirrors R_1 and R_2, respectively. The electron concentration in InSb was assumed to be $N_e = 1\cdot10^{18}$ cm^{-3}. Due to the low value of the electron effective mass, doped InSb has sufficiently high magneto-optical properties in the MWIR and LWIR regions ($\lambda >$ μm). KBr and Ge are widely used IR optical materials.

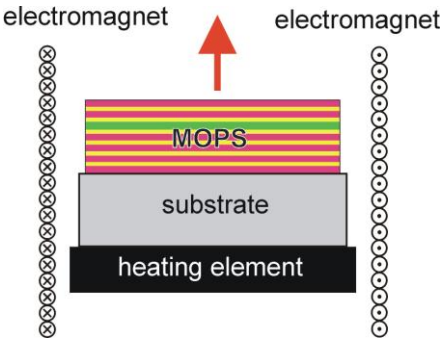

Fig. 5. Schematic of IR emission source with dynamically tunable spectrum.

The emitter is placed inside a variable magnetic field source (in this case, it is an electromagnet) in such way that the direction of the magnetic field is perpendicular to the structure.

The following values of the material refractive indices were used in the calculations: $n_{Ge} = 4$, $n_{KBr} = 1.54$ [20] and the dispersion of the complex refractive index of leucosapphire $N_{Al_2O_3}(\lambda) = 1.54 + 0.4\lambda^2/\left(\lambda^2 - 12.62^2\right) + i\,0.026\lambda$ as obtained by approximating the tabular data [21]. For doped InSb, the complex refractive index dispersion law $N_{InSb} = \sqrt{\varepsilon_\infty\left(1 - \lambda^2/\lambda_p^2\right)} + i\lambda\alpha/4\pi$ was used, where c is the speed of light in vacuum, $\lambda_c = 2\pi m_e^* c/eH$, $\lambda_p = c\sqrt{\varepsilon_\infty m_e^*/N_e e^2}$, $\varepsilon_\infty = 15.68$ [22] is the high frequency dielectric constant, $m_e^* = 0.03m$ [22] is the electron effective mass, m is the electron mass, e is the electron charge, and $\alpha = 3\cdot10^{-20} N_e\cdot\lambda^3$ is the absorption coefficient by free electrons, the spectral dependence of which was obtained from the data [23]. We used the thicknesses of the Ge, KBr and *n*-InSb layers equal to 0.563, 1.47 and 5 μm, respectively.

Fig. 6a shows the emission spectra of the source without magnetic field (curve *1*) and in the magnetic field of 5 kOe (curve *2*) and 25 kOe (curve *3*). The presented spectral region corresponds to the photonic band gap of MOPS with high reflection coefficients of the mirrors ($R_1 \approx 0.91$, $R_2 \approx 0.99$). As can be seen from this figure, the emission spectrum contains three emission lines, which split when the magnetic field is applied. The amplitude of the zero-field lines is close to the emission intensity of the blackbody. The width of the emission lines ranges from $2.3\cdot10^{-2}$ μm (at the shortwave end of the region) to $1.34\cdot10^{-1}$ μm (at the longwave end of the region).

The dependence of the spectral positions of the lines on the magnetic field strength is shown in Fig. 6b. It can be seen from this figure that the lines of the P^- and P^+ components with adjacent interference orders shift toward each other. At the wavelength $\lambda \approx 13.85$ μm, two lines merge at the magnetic field $H \approx 18$ kOe. When the field is further increased, the merged line splits again.

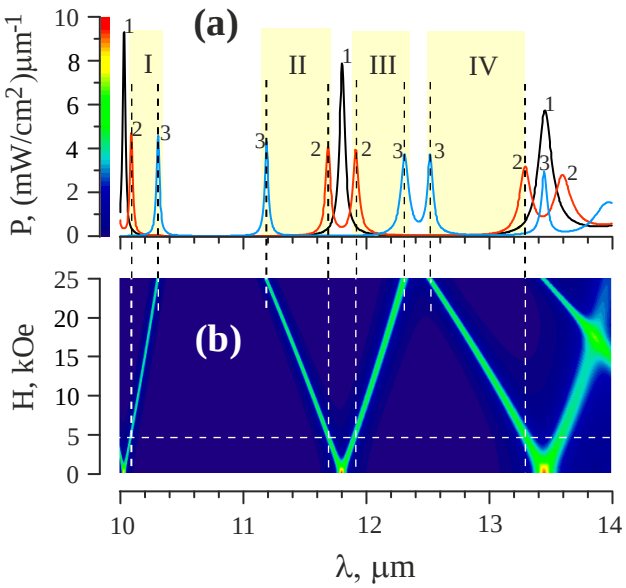

Fig. 6. (a) Calculated emission spectra of the IR source based on the $(Ge/Kbr)^2InSb/(KBr/Ge)^4$ structure at the magnetic field values: *1* – $H = 0$, *2* – 5 kOe, *3* – 25 kOe. I, II, III and IV are the spectral regions of a smooth tuning of the source emission line position; (b) 3D plot of the emission lines shift with increasing magnetic field. The MOPS temperature was assumed to be 400 K.

Four spectral regions are selected, in which smooth tuning of the source emission spectrum is observed. Under the stability condition of the line amplitude and at achievable magnetic fields ($H \le 25$ kOe), these regions are: 10.09…10.3 μm (I), 11.19…11.69 μm (II), 10.92…12.31 μm (III) and 12.52…13.29 μm (IV). Although these regions are not too wide, their widths are sufficient, *e.g.*, to perform spectral analysis of a gas absorption line in an optical gas analyzer.

4.2. Emission source with amplitude modulation of emission intensity

A design of the IR emission source with amplitude modulation of emission intensity, which can be implemented in practice, is shown schematically in Fig. 7. Its emitter is a combination of a emitting MOPS with a photonic structure whose transmission line coincides with the spectral position of the zero-field emission line. The MOPS is a $(ZnSe/KBr)^2/InSb/Al$ structure, the back mirror of which is formed by an Al layer. The used thicknesses of the ZnSe, KBr and *n*-InSb layers were assumed to be 1.017, 1.594 and 29.69 μm, respectively. The electron concentration in *n*-InSb used was $N_e = 2\cdot10^{18}$ cm^{-3}. PS is a $(ZnSe/KBr)^5/(KBr/ZnSe)^6$ multi-layered structure with the thicknesses of the ZnSe and KBr layers of 1.017 and 1.594 μm, respectively. MOPS and PS are separated by an incoherent KF layer. The following values of the refractive indices were used in the calculations: $n_{ZnSe} = 2.41$ and $n_{KF} = 1.31$ [20].

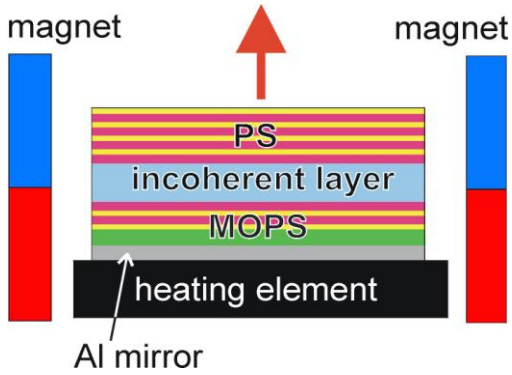

Fig. 7. Schematic of the IR emission source with amplitude modulation of intensity.

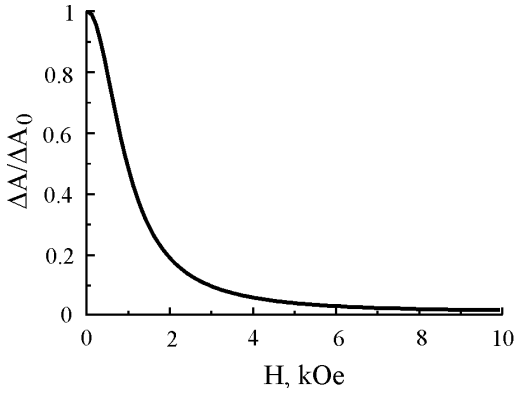

Fig. 9. Dependence of the line height on magnetic field strength.

Dispersion of the Al complex refractive index $N_{\mathrm{Al}} = -13.19 + 3.84\lambda + i(20.23 + 6.9\lambda)$ was used as obtained by approximation of the tabular data [20].

This design uses a moving permanent magnet as a variable magnetic field source. It should be noted that modern neodymium magnets have sufficiently strong magnetic fields. The strength of the magnetic field passing through the MOPS is changed by moving the magnet relative to the emitter.

Fig. 8 shows the emission spectra of the source at different magnetic field values. It can be seen from this figure that the emission spectrum of the source is a narrow line. The parameters of the MOPS layers were chosen in such way that the amplitude of the zero-field line is almost equal to the emission intensity of the blackbody, its width is 0.025 μm and its spectral position is at 9.8 μm. After application of magnetic field the line height decreases. The intensity of the source emission becomes almost equal to zero at H = 10 kOe.

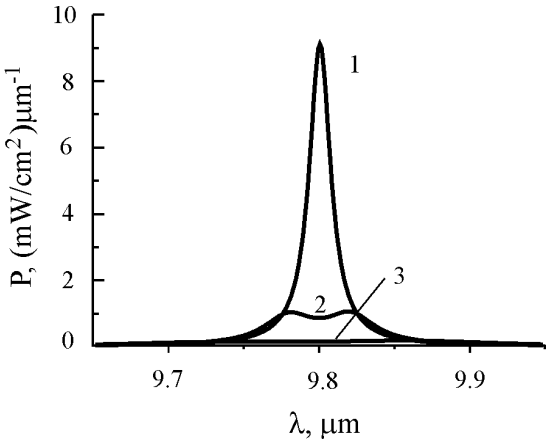

Fig. 8. Calculated emission spectra of the IR source based on the $(ZnSe/KBr)^5/(KBr/ZnSe)^6$/(incoherent KF layer)/$(ZnSe/KBr)^2$/InSb/Al structure: *1* – H = 0, *2* – 3 kOe, *3* – 10 kOe. The MOPS temperature was assumed to be 400 K.

Fig. 9 shows the dependence of the line height on magnetic field strength. In this figure, the line height is normalized to the height of the zero-field line. It can be seen that ΔA rapidly decreases with increasing H.

Note that the spectral position of the source emission line coincides with the position of the absorption line of ozone and gaseous ammonium (λ = 9.8 μm). Therefore, such source can be used in optical devices for detecting and measuring concentrations of these gases in the atmosphere or in other gas mixtures.

5. Conclusions

The paper shows that one-dimensional magneto-optical photonic structures may be used as the narrow-band controllable emission sources of mid- and far-wavelength IR emission. Influence of the composition and design features of the structure on both the spectral and amplitude characteristics of its thermal radiation and on the possibility of controlling them by an external magnetic field has been studied. Based on the obtained results, the useful recommendations for creating such sources were given.

The designs of two magnetically controllable narrow-band sources of IR emission with controllable spectral characteristic and with amplitude modulation of intensity have been presented. The sources consist of dielectric optical material layers and a A^3B^5 semiconductor compound layer as a magneto-active one. As theoretical modeling showed, MOPS based on A^3B^5 semiconductor compounds demonstrate dynamic changes of the emission parameters at achievable magnetic fields and can be implemented in practice.

Application of such narrow-band controllable sources of IR emission in optical devices makes it possible to exclude dispersive elements (optical filters, prisms, diffraction gratings) and amplitude modulators. They can be used in the gas analyzers, optical devices for determining the composition of substances and identifying organic compounds, for calibrating IR receivers and optical systems in narrow spectral ranges, in detection systems of thermal objects *etc*.

Acknowledgement

The work was carried out in the framework of the theme "Development and creation of new functional materials, study of their physical properties and influence of production technologies and external factors on them with the aim of creating an elemental base for the needs of electronic and sensor technology" financed by the National Academy of Sciences of Ukraine.

References

1. Al-Saymari F.A., Craig A.P., Lu Q. *et al.* Mid-infrared resonant cavity light emitting diodes operating at 4.5 μm. *Opt. Exp*. 2020. **28**, No 16. P. 23338–23353. https://doi.org/10.1364/OE.396928.
2. Muhowski A.J., Bogh C.L., Heise R.L. *et al*. performance of mid-infrared superlattice light emitting diodes grown epitaxially on silicon. *J. Cryst. Growth*. 2019. **507**. P. 46–49. https://doi.org/10.1016/j.jcrysgro.2018.10.047.
3. Lin Y., Suchalkin S., Kipshidze G. *et al.* Effect of hole transport on performance of infrared type-II superlattice light emitting diodes. *J. Appl. Phys*. 2015. **117**. P. 165701. 10.1063/1.4919070.
4. Das N.C., Bradshaw J., Towner F., Leavitt R. Long-wave (10 μm) infrared light emitting diode device performance. *Solid State Electron*. 2008. **52**, No 11. P. 1821–1824. https://doi.org/10.1016/j.sse.2008.09.003.
5. Aziz M., Xie C., Pusino V. *et al.* Multispectral mid-infrared light emitting diodes on a GaAs substrate. *Appl. Phys. Lett.* 2017. **111**. P. 102102 (1–5). https://doi.org/10.1063/1.4986396.
6. Das N.C. Infrared light emitting device with two color emission. *Solid-State Electron*. 2010. **54**, No 11. P. 1381–1383. https://doi.org/10.1016/j.sse.2010.06.007.
7. Malyutenko V.K., Bolgov S.S., Malyutenko O.Yu. Above-room-temperature 3–12 μm Si emitting arrays. *Appl. Phys. Lett*. 2006. **88**. P. 211113 (1–3). https://doi.org/10.1063/1.2207833.
8. Malyutenko V.K., Bogatyrenko V.V., Malyutenko O.Yu., Chyrchyk S.V. Si infrared pixelless photonic emitter. *Proc. SPIE*. 2005. **5957**. P. 75–81. https://doi.org/10.1117/12.622104.
9. Gao X., Cathelinaud M., Zhang X., Ma H., Liu Z. Spontaneous emission enhancement based on thin-film chalcogenide/fluoride one dimensional photonic crystal. *Opt. Mater.* 2022. **130**. P. 112587. https://doi.org/10.1016/j.optmat.2022.112587.
10. Umar A., Jiang C. Manipulation of thermal radiation by using photonic crystals. *Int. J. Mod. Phys. B*. 2021. **35**. P. 2150262. https://doi.org/10.1142/S0217979221502623.
11. Maslov V.P., Morozhenko V.O., Kachur N.V. Features of thermal radiation of one-dimensional photonic structures on an absorbing substrate. *SPQEO*. 2021. **24**. P. 444–449. https://doi.org/10.15407/spqeo24.04.444.
12. Costa C.H., Vasconcelos M.S., Fulco U.L., Albuquerque E.L. Thermal radiation in one-dimensional photonic quasicrystals with graphene. *Opt. Mater*. 2017. **72**. P. 756–764. https://doi.org/10.1016/j.optmat.2017.07.029.
13. Pühringer G., Jakoby B. Modeling of a highly optimizable vertical-cavity thermal emitter for the mid-infrared. *Procedia Eng.* 2016. **168**. P. 1214–1218. https://doi.org/10.1016/j.proeng.2016.11.419.
14. Singh L., Qiu E., Cardin A.E. *et al.* Controlling thermal radiation with a phase-change metasurface. *Proc. Conf. on Lasers and Electro-Optics (CLEO)*. San Jose, CA, USA, 15–20 May, 2022. https://doi.org/10.1364/CLEO_QELS.2022.FTh4D.1.
15. Du K.-K., Li Q., Lyu Y.-B. *et al.* Control over emissivity of zero-static-power thermal emitters based on phase-changing material GST. *Light: Sci. Appl*. 2017. **6**. P. 1–7. https://doi.org/10.1038/lsa.2016.194.
16. Taylor S., Long L., McBurney R., Sabbaghi P., Chao J., Wang L. Spectrally-selective vanadium dioxide based tunable metafim emitter for dynamic radiative cooling. *Sol. Energy Mater Sol. Cells.* 2020. **217**. P. 110739. https://doi.org/10.1016/j.solmat.2020.110739.
17. Coppens Z.J., Valentine J.G. Spatial and temporal modulation of thermal emission. *Adv. Mater*. 2017. **29**. P. 1701275 (1–6). https://doi.org/10.1002/adma.201701275.
18. Pipa V.I., Liptuga A.I., Morozhenko V.O. Thermal emission of one-dimensional magnetophotonic crystals. *J. Opt.* 2013. **15**. P. 075104 (1–6). https://doi.org/10.1088/2040-8978/15/7/075104.
19. Liptuga A., Morozhenko V., Pipa V., Venger E., Kostiuk T. Faraday-active Fabry–Perot resonator: Transmission, reflection, and emissivity. *J. Opt. Soc. Am. A*. 2012. **29**. P. 790–796. https://doi.org/10.1364/JOSAA.29.000790.
20. Weber M.J. *Handbook of Optical Materials*. Boca Raton, CRC Press, 2003.
21. Whitson E.M., Jr. *Handbook of the Infrared Optical Properties of Al_2O_3, Carbon, MgO, and ZrO_2*. Vol. 1. Aerospace Corporation, 1975.
22. Madelung O. *Semiconductors: Data Handbook*. Springer, 2003.
23. Ukhanov Yu.I. *Optical Properties of Semiconductors*. Moscow, Nauka, 1977 (in Russian).

Authors' contributions

Venger E.F.: project administration, resources, supervision, validation, discussion of the results, writing – review & editing.

Morozhenko V.O.: conceptualization, investigation, calculation, analysis, data curation, writing – original draft, writing – review & editing, visualization.

Authors and CV

Evgen Fedorovich Venger, Doctor of Physical and Mathematical Sciences, Professor, Corresponding Member of NAS of Ukraine. Head of the Department of sensor systems, V. Lashkaryov Institute of Semiconductor He is the author of more than 500 scientific publications, 40 patents, 24 textbooks and manuals. The area of his scientific interests includes physics and technology of semiconductor materials, hetero- and hybrid structures and devices (thin film solar cells, photoresistors, new types of photoconverters, *etc*.), as well as analysis, diagnostics, modeling and predicting physical processes in different objects.
E-mail: vengeref@gmail.com,
https://orcid.org/0000-0003-1508-1627

Vasyl Oleksandrovych Morozhenko, PhD in Physical and Mathematical Sciences, Senior Researcher at the Department of sensor systems, V. Lashkaryov Institute of Semiconductor Physics, NAS of Ukraine. He is the author of more than 50 scientific publications and 14 patents. The area of his scientific interests includes infrared spectroscopy, optical properties of semiconductors, photonics and magnetophotonics.
E-mail: morozh@meta.ua,
https://orcid.org/0000-0001-7834-2260

Вузькосмугові керовані джерела ІЧ випромінювання на основі одновимірних магнітооптичних фотонних структур

Є.Ф. Венгер, В.О. Мороженко

Анотація. Створення керованих вузькосмугових джерел випромінювання середнього та далекого інфрачервоного діапазонів є одним із першочергових завдань інфрачервоної техніки. У роботі запропоновано та продемонстровано нелюмінесцентні (теплові) магнітокеровані джерела інфрачервоного випромінювання на основі напівпровідникових магнітооптичних фотонних структур (МОФС). Показано, що інтерференційні ефекти зумовлюють вузькосмуговий спектр їх теплового випромінювання, а магнітне поле дає змогу ефективно керувати спектральними та амплітудними параметрами випромінювальної здатності в середньохвильовому та довгохвильовому інфрачервоному діапазонах. Досліджено вплив складу та конструктивних особливостей МОФС на емісійні характеристики джерела. На основі отриманих результатів запропоновано конструкції джерел на основі напівпровідників A^3B^5 з динамічно перестроюваним спектром та амплітудною модуляцією випромінювання. Теоретичне моделювання показало можливість динамічного керування параметрами їх випромінювання за допомогою реально досяжного магнітного поля. Такі джерела можуть бути використані в системах моніторингу довкілля, медицині, криміналістиці, інфрачервоній спектроскопії тощо.

Ключові слова: інфрачервоні джерела, магнітооптичні фотонні структури, теплове випромінювання, випромінювальна здатність.